Vibrational and electronic excitations in the (Ce,La)MIn$_5$ (M=Co,Rh) heavy-fermion family

H. Martinho,[1] P. G. Pagliuso,[2] V. Fritsch,[3] N. O. Moreno,[4] J. L. Sarrao,[3] and C. Rettori[2]
[1]*Instituto de Pesquisa e Desenvolvimento, UNIVAP, 12244-050, São José dos Campos, São Paulo, Brazil*
[2]*Instituto de Física "Gleb Wataghin," UNICAMP, 13083-970, Campinas, São Paulo, Brazil*
[3]*Los Alamos National Laboratory, Los Alamos, New Mexico 87545, USA*
[4]*Departamento de Física, Universidade Federal de Sergipe, São Cristovão-SE CEP 49100-000, Brazil*
(Received 10 November 2006; revised manuscript received 17 May 2006; published 5 January 2007)

We present a systematic study at ambient pressure of the phononic and electronic Raman-active excitations in the *ab* plane of the (Ce,La)MIn$_5$ (M=Co,Rh) heavy-fermion family. We found that the characteristic Raman spectra of this family of compounds display two phonon modes at ~38 and ~165 cm^{-1} and a broad electronic background centered at ~40 cm^{-1}. For CeCoIn$_5$, the temperature dependence of these excitations shows anomalous behavior near T^*=45 K that may indicate a nontrivial renormalization of the electronic structure driven by strong correlations between hybridized 4f electrons.

DOI: 10.1103/PhysRevB.75.045108 PACS number(s): 75.20.Hr, 71.27.+a, 72.15.Qm, 78.30.−j

I. INTRODUCTION

At the heart of heavy-electron physics lies the microscopic understanding of how localized f electrons at high T evolve to itinerant heavy quasiparticles in a low-T metallic state. The fundamental mechanism of this evolution involves the Kondo coupling between f electrons and conduction electrons.[1] However, despite the reasonable understanding of isolated Kondo impurity physics given by the single-impurity model (SIM),[2] the problem of a lattice of Kondo impurities does not have a general solution. The Kondo lattice model (KLM),[3] a strong-coupling limit of the SIM, represents a partly successful approach to this problem that can explain within some limits the magnetic and transport properties of Kondo lattices.[4,5] However, this model neglects spin-spin interactions and fails when heavy-electron magnetic correlations become important (e.g., near to magnetic ordering).

Recently, a new picture of remarkable simplicity has been proposed as the low-T solution of the Kondo lattice. It was developed based on studies of specific heat, electrical resistivity,[6] and NMR (Ref. 7) in the 1-1-5 family of heavy-fermion (HF) materials CeMIn$_5$ (M=Rh,Ir,Co).[8] These materials, in particular CeCoIn$_5$, have been the focus of intense investigations due to their amazing physical properties such as heavy-fermion superconductivity, quantum criticality, and non-Fermi-liquid behavior.[8–10] According to this new picture, below the crossover temperature T^*, the noninteracting Kondo impurities in the so-called Kondo-gas (KG) state partially condense into a coherent interacting heavy-electron liquid, giving rise to the Kondo-liquid (KL) state.[6] Below T^* there is coexistence of both phases with the relative fraction of KL, ϕ, playing the role of an order parameter. It was shown[6] that the magnetic electronic scattering represented by the T dependence of the resistivity of CeCoIn$_5$ can be well described by the product of $(1-\phi)$ and the resistivity of the single Kondo impurity. T^* was found to be ~45 K for CeCoIn$_5$ and ~8 K for CeRhIn$_5$.[7] The KG-KL model differs significantly from the KLM in the sense that it proposes the survival *side by side* of a single and a dense lattice of Kondo impurity excitations. A microscopic experimental hallmark of such a scenario would be the manifestation of these two different components coexisting at low T. In spite of its simplicity, this phenomenological model does not represent a consensus and does not furnish any new microscopic understanding about the heavy-fermion physics. Thus, more experimental and theoretical efforts are needed to solve the problem of a lattice of Kondo impurities. In this work we present a Raman scattering report on the 1-1-5 heavy-fermion family. We investigate the T dependence of the Raman spectra of CeCoIn$_5$ and its reference compound LaCoIn$_5$, comparing their behavior with that expected by the SIM.

II. EXPERIMENTAL DETAILS

Large platelike single crystals of RCoIn$_5$ (R=Ce,La) were grown as reported previously.[8] The inset of Fig. 1 presents a picture of a monocrystal of CeCoIn$_5$ and the crystallographic a, b, and c axes. The unit cell of this compound belongs to the tetragonal $P4/mmm$ space group and for this symmetry four phonons $A_{1g}+B_{1g}+2E_g$ are expected to be

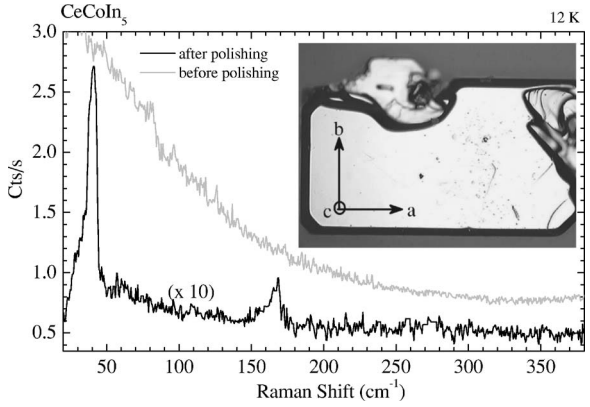

FIG. 1. Raman spectra of polished and unpolished monocrystals of CeCoIn$_5$ at 12 K. The spectral intensity of the polished crystal was multiplied by 10 for clarity. The inset shows a picture of a monocrystal of CeCoIn$_5$. The a, b, and c crystallographic axes are also indicated.

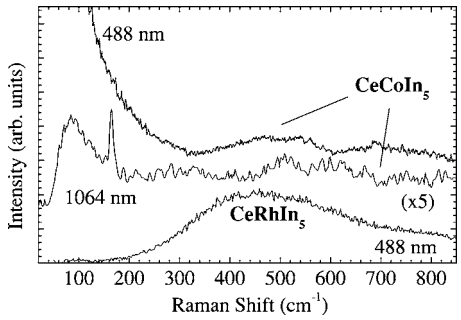

FIG. 2. Raman spectra at 300 K measured the as-grown surfaces of CeMIn$_5$ samples (M=Co,Rh) excited by 488 and 1064 nm laser lines. The spectral intensity at 1064 nm was multiplied by a factor of 5 for clarity.

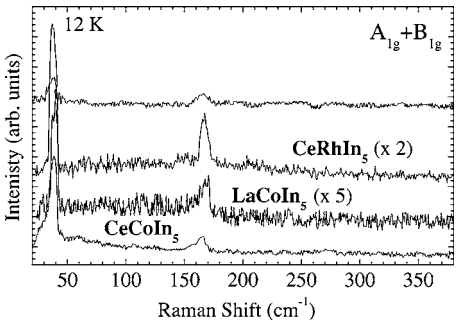

FIG. 3. Raman spectra at 12 K in the polished surfaces of RMIn$_5$ samples (R=La,Ce) in the $A_{1g}+B_{1g}$ symmetry. The spectra of CeRhIn$_5$ and LaCoIn$_5$ were multiplied by 2 and 5, respectively, and vertically translated for clarity.

Raman active. All these modes involve motion of In atoms at sites of symmetry *Rmm* (basal plane). The Raman measurements were carried out using a triple spectrometer with a liquid nitrogen charge-coupled device detector. The spectra were corrected by the spectrometer response obtained measuring the emission of a tungsten lamp and comparing it with the emissivity of a blackbody at the same T. The 488.0 nm line of an Ar^+ ion laser was used as excitation source. The laser power at the sample was kept below 12 mW on a spot radius of about 50 μm. The samples were cooled in a cold finger of a He closed-cycle Displex cryostat, and measured in a near-backscattering configuration on the *ab* plane. One set of measurements at 300 K was made using a Fourier transform (FT) Raman spectrometer operating at 1064 nm (Fig. 2). The laser power in this case was 200 mW on a spot of 250 μm radius. The A_{1g} and B_{1g} phonons could be observed in both the *ab* or *ac* planes while the E_g phonon is observable only in the *ac* or *bc* plane. The choice of the (a,a) geometry probes a combination of the A_{1g} and B_{1g} symmetries; the (a',b') geometry couples to excitations of B_{1g} symmetry, while choosing the (a,b) geometry probes the B_{2g} symmetry. a' (b') denote axes rotated by 45° from the crystallographic a (b) axes. Due to the well-known problem of In flux surface contamination in these crystals, all spectra were obtained on mechanically polished samples using diamond paste with grain sizes of 0.05 μm.

III. RESULTS AND DISCUSSION

Figure 1 presents the raw Raman signal of a CeCoIn$_5$ crystal at 12 K before and after polishing. In the polished crystal one is able to observe two Raman modes at 38 and 165 cm^{-1} and a broad electronic background centered at 40 cm^{-1}, while the unpolished crystal presents only a central broad peak. This illustrates the crucial role that a high-quality sample surface plays in a Raman experiment. Similar polishing procedures were applied to CeMIn$_5$ and related materials for resistivity, x-ray magnetic diffraction, and photoemission experiments.

Figure 2 presents the Raman spectra at 300 K obtained from as-grown unpolished surfaces of CeMIn$_5$ samples (M=Co,Rh) excited by 488 and 1064 nm (FT Raman) laser lines. The Raman spectrum of CeCoIn$_5$ excited by the 488 nm line presents a broad central mode that disappears in the FT Raman spectra excited by 1064 nm. This central mode also disappears with polishing as seen in Fig. 1. Due to the smaller penetration depth of the light at 488 nm ($\sim$1/5 of that at 1064 nm as estimated from the reflectivity data[11] on CeCoIn$_5$) the Raman scattering signal at this wavelength will be more sensitive to surface effects. The peak at $\sim$165 cm^{-1} is present in both the as-grown crystals at 1064 nm (Fig. 2) and polished samples at 488 nm (Fig. 1). This fact corroborates the intrinsic origin of this mode.

Figure 3 presents the Raman spectral function Im χ for the RMIn$_5$ samples (R=La,Ce; M=Co,Rh) in the $A_{1g}+B_{1g}$ symmetry at 12 K. Im χ is defined as the raw data divided by the Bose-Einstein thermal population factor $[n(\omega,T)+1]$. The spectra of CeRhIn$_5$ and LaCoIn$_5$ were multiplied by 2 and 5, respectively, and vertically translated for clarity. For all samples we observe two peaks at $\sim$38 and $\sim$165 cm^{-1}. In CeCoIn$_5$ we observe a broad electronic background centered at 40 cm^{-1}. In fact, a closer inspection of the LaCoIn$_5$ and CeRhIn$_5$ spectra also indicates the presence of a low-intensity electronic background centered at $\sim$40 cm^{-1}. These results indicate that the two phonons and the electronic background define the expected Raman spectra of the 1-1-5 compounds.

The phonon peak at $\sim$165 cm^{-1} for R=La and Ce presents an asymmetric Fano line shape, indicating interference between conduction electrons and phonon wave functions implying strong electron-phonon coupling.[12] This fact could be used to probe the evolution of the electronic interactions and hybridization effects in CeCoIn$_5$ using LaCoIn$_5$ as a reference.

Figure 4 displays the raw polarized Raman spectra for CeCoIn$_5$ at 12 K. (Data in the *ac* plane were not reliable due to difficulties in obtaining a good crystal surface for this orientation.) From these data we conclude that the phonon at 165 cm^{-1} has A_{1g} symmetry. The mode at 38 cm^{-1} is always present independent of polarization, implying either a defect-induced mode or a strong E_g mode appearing due to the lack of polarization due to strain or small crystal misalignment. We will label it as the E^* mode. The fact that this mode appears around the same frequency for different crystals is a strong indication of its intrinsic origin. We also notice that the electronic background is isotropic.

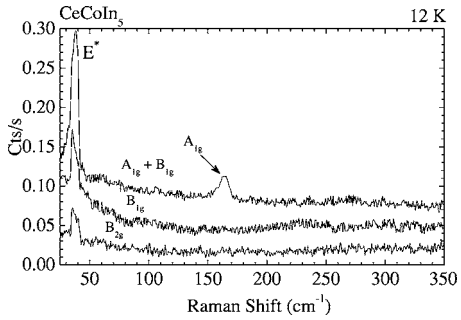

FIG. 4. Polarized Raman spectra at 12 K for $CeCoIn_5$.

In order to study the T evolution of phonons and electronic excitations we measured the T dependence of the Raman spectra in the $A_{1g}+B_{1g}$ symmetry for both compounds.

For $LaCoIn_5$ we found that the Raman spectra are nearly T independent. Figure 5 shows some selected spectra for $LaCoIn_5$ at 12, 60, and 300 K that illustrate this fact.

Selected spectra for $CeCoIn_5$ at 12, 25, 50, and 300 K are shown in Fig. 6(a). At first glance we note the fast decrease of the E^* phonon intensity and the broadening of the A_{1g} mode with increasing T. It is worth noting that we see no evidence for the opening of a hybridization gap at ~75 meV (600 cm^{-1}) below 100 K as found by optical conductivity,[11] indicating that the electronic excitations sampled by optical conductivity may be Raman inactive.

We performed a more detailed analysis of our data by fitting the Raman spectral function to the expression

$$\mathrm{Im}\,\chi = A_0\frac{\omega\Gamma_e}{\omega^2+\Gamma_e^2} + \frac{A_1}{\omega\sqrt{\pi/2}}e^{-2(\omega-\omega_1)^2/\Gamma_1^2} + A_2\frac{(q+\epsilon)^2}{1+\epsilon^2}, \tag{1}$$

where $\epsilon=(\omega-\omega_2)/\Gamma_2$.

The first term corresponds to the electronic impurity scattering background. It is related to the scattering of light-excited electron-hole pairs[13] by impurities, with a scattering rate Γ_e. Γ_e is closely related to the transport lifetime.[13] The second term is a Gaussian function centered at ω_1 with linewidth Γ_1 used to reproduce the line shape of the E^* peak. The last term is a Fano line shape.[12] The parameter q represents the Fano asymmetry and it is inversely proportional to the electronic density of states $q\sim 1/\rho$. ω_2 is the phonon

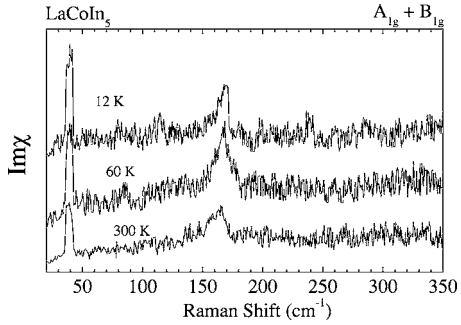

FIG. 5. Raman response Im χ for $LaCoIn_5$ at 12, 60, and 300 K.

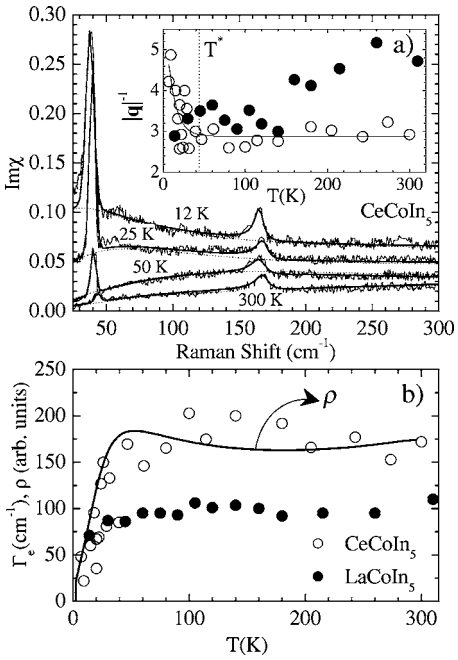

FIG. 6. (a) Raman spectra at 12, 25, 50, and 300 K for $CeCoIn_5$ in the $A_{1g}+B_{1g}$ symmetry. The solid lines correspond to the fitting using Eq. (1). The dotted lines represent the electronic impurity scattering background given by the first term of Eq. (1). The inset shows the T dependence of the Fano asymmetry parameter $|q|^{-1}$ for $CeCoIn_5$ and $LaCoIn_5$. (b) The T dependence of the electron-impurity scattering relaxation time Γ_e for $CeCoIn_5$ and $LaCoIn_5$. The solid line represents the electrical resistivity data for $CeCoIn_5$.

energy and Γ_2 its linewidth. A_0, A_1, and A_2 are adjustable parameters. The Fano resonance is related to the interference between discrete and continuum of states. In the Raman scattering the Fano effect appears due to interference between the discrete phonon state and the electronic continuum. The resonance manifests itself in the spectra as an asymmetry of the otherwise symmetrical Lorentz line shape as well as shifting the otherwise unperturbed phonon energy. The asymmetry factor is given by

$$q = \frac{f_1 T_p/T_e - E_0 - \omega_0}{\pi^2 f_1^2 \rho(E)}. \tag{2}$$

It depends on the conduction-electron–phonon interaction f_1; the matrix element of the Raman tensor between phonon and ground states $T_p=\langle\text{phonon}|T|\text{ground}\rangle$; the matrix element of the Raman tensor between continuum and ground states $T_e=\langle\text{continuum}|T|\text{ground}\rangle$; the unperturbed phonon energy E_0; the phonon energy ω_0; and the conduction electrons density of states $\rho(E)$. Thus, the Fano resonance present in the Raman spectra could be used to indirectly probes excitations in the electronic continuum.

The solid lines in Fig. 6(a) correspond to fitting to Eq. (1) while the dotted lines correspond to electronic impurity scattering background given by the first term of Eq. (1). The agreement between fitted and experimental curves is evident. In the inset of Fig. 6(a) we show the T dependence of $|q|^{-1}$ for $(La,Ce)CoIn_5$. For $CeCoIn_5$ one observes an exponential

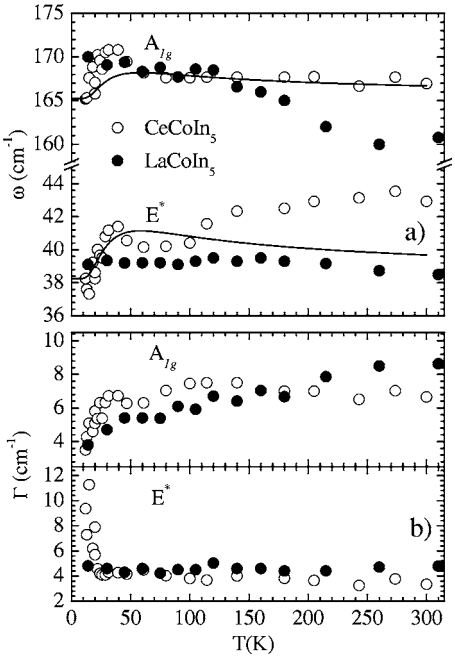

FIG. 7. T dependence of the A_{1g} and E^* phonon frequencies (a) and linewidth (b). The solid lines are simulations of Nayak *et al.*'s theory (Ref. 16).

decrease of $|q|^{-1}$ near T^*. The solid line is a fitting to $\sim e^{-T_0/T}$ which furnishes $T_0=8$ K. It is important to notice that the exponential decay of the T dependence of $|q|^{-1}$ is similar to the linewidth behavior of the E^* mode due to the common origin of both effects. On the other hand, the T dependence of $|q|^{-1}$ for $LaCoIn_5$ is very different. It increases with T and does not display any singularity or change of slope for $10<T<300$ K. This fact indicates that the A_{1g} phonon has special sensitivity to the hybridized state of $CeCoIn_5$. In Fig. 6(b) we present the T dependence of Γ_e for R=Ce and La. For R=Ce, within experimental error, Γ_e is nearly T independent at high T, showing a significant drop for $T \lesssim 50$ K. In fact, Γ_e qualitatively follows the resistivity behavior (solid line) for R=Ce while Γ_e is constant (or slightly metalliclike) for R=La.

Figure 7(a) shows the T dependence of the frequencies ω of the A_{1g} and E^* modes for R=Ce and La samples. For R=Ce we found an anomalous maximum near $T^*=45$ K in the frequency of both phonons. Typically, phonons harden on cooling as result of lattice contraction, resembling the T dependence of the A_{1g} phonon for R=La [Fig. 7(a)], or may present a nearly constant behavior, like the E^* phonon of R=La [Fig. 7(a)] whether or not their Grüneisen parameter is small. The T dependence of the linewidth Γ for A_{1g} and E^* modes of both samples is presented in Fig. 7(b). The A_{1g} modes for R=Ce and La present roughly the same smooth broadening when T is increased as expected considering lattice thermal anharmonicity.[14] However, within our experimental resolution we could not observe any anomaly in $\Gamma(A_{1g})$ near T^*. On the other hand, the E^* mode for R=Ce shows a strong broadening for $T<T^*$ (the linewidth of this mode for R=La is nearly T independent).

As the electronic and phononic excitations in $LaCoIn_5$ present the expected behavior for their frequency and linewidth as function of temperature, we associate the observed anomalous features seen in the T dependence of the Raman spectra of $CeCoIn_5$ with its f electrons.

As such, the strong broadening of the $CeCoIn_5$ E^* mode for $T<T^*$ could be associated with an increase in the number of decay channels due to hybridization effects near T^*. In fact, the $4f$ electrons become more itinerant[15] for $T<T^*$ due to their hybridization with the conduction band, producing an enhancement of the electronic density of states. This result is consistent with the T dependence of the q parameter of the A_{1g} mode for $CeCoIn_5$ [Fig. 6(a)], which exponentially decreases below T^*. The fact that the linewidth of the E^* mode is particularly affected by electronic changes at T^* may be explained by considering that its energy is close to the energy scale of the heavy-electron condensation $\hbar\omega(E^*)/k_BT^* \sim 1.2$.

Another peculiar aspect of the E^* mode is the significant increase of its intensity when T is lowered (the same occurs for A_{1g} but less pronounced) for $CeCoIn_5$ while it is nearly T independent for $LaCoIn_5$. For the Ce-based compound, the E^* mode intensity increases roughly exponentially when temperature is lowered from 300 to 12 K. This behavior is not restricted to $T<T^*$.

Turning now to the T dependence of the $CeCoIn_5$ electronic Raman scattering it is important to notice that the qualitative scaling between Γ_e and the electrical resistivity of $CeCoIn_5$ [see Fig. 6(b)] could only be fully understood within a quantitative microscopic relaxation model of the Kondo lattice. However, one could argue that, as for the resistivity,[6] the decrease of Γ_e could be due to the disappearance of isolated Kondo centers which condense into a cooperative liquid phase at T^*. The phenomena described above involving the T dependence of Γ_e, the q parameter of the A_{1g} mode, and the linewidth of the E^* mode may be speculated to be a simultaneous manifestation of the two KG and KL phases coexisting side by side as proposed in the KG-KL scenario.[6] However, additional experimental work such as the study of these features in the Raman data as a function of pressure and/or doping is required to confirm this hypothesis.

Another aspect of the low-T Kondo lattice phase in $CeCoIn_5$ is the importance of inter-site magnetic correlations and quantum criticality.[6,10] Nayak *et al.*[16] has proposed a theory to explain the phonon response in HF systems within the SIM, but apart from its simplicity, this theory has reproduced the general experimental trends of many Kondo lattice materials such as $CeAl_3$, UPt_3, and $CeRu_2Si_2$.[16] This model evaluates the contributions to the phonon self-energy from the mixing between the f and conduction electrons as well as from the f electrons alone in the presence of on-site Coulomb repulsion. However, this model neglects the effects of the f-f magnetic correlations in the electronic continuum. In the case of $CeCoIn_5$ it will be illustrative to compare our data to the expected behavior of phonons given by the Nayak model.

To quantitatively test Nayak's theory[3,16] we have performed numerical simulations of the T dependence of ω for the A_{1g} and E^* modes of $CeCoIn_5$. It depends on six parameters g, r, E_0, V, U, and W, defined below. The simulated curves are shown as solid lines in Fig. 7(a) and were obtained from theory of Nayak *et al.*[16] All parameters, except g,

are the same for both phonons. Most of the parameters were to set to their values extracted by independent techniques from the literature, except g and r.

The parameter g corresponds to the dimensionless effective coupling constant between hybridized electrons and phonons and is given by $g=N(0)f_1^2/\hbar\omega$ where $N(0)$ is the density of states at the Fermi level and f_1 is the energy of interaction between conduction electrons and phonons. The best simulation was obtained for $g_{A_{1g}}=0.04$ and $g_{E^*}=g_{A_{1g}}\omega_{A_{1g}}/\omega_{E^*}=0.175$. The main effect of this parameter is change the strength of the softening. In order to get a comparative value we can estimate a lower limit for g from the Fano linewidth Γ of the A_{1g} mode. Γ is a function of f_1 and the density of electronic excitations, ρ, $\Gamma=2\pi f_1^2\rho$.[12] Overestimating ρ by $N(0)$, using Γ values from Fig. 7(b) and $N(0)=10.8$ eV^{-1} from Ref. 17 we found $f_1\sim 3$ meV and $g\gtrsim 4\times 10^{-3}$. An upper limit could be estimated by considering the extreme case in which the average energy of the hybridized electrons is equal to the phonon energy, implying $g=1$. The parameter r corresponds to the ratio between the phonon coupling constant to f electrons, f_2, and f_1. Razafimandiby *et al.*[18] have shown that the condition $r<1$ is always observed. E_0 and W are the positions of the f level relative to the Fermi level and the conduction band width, respectively. We use the value of 0.1 eV at the Γ point for both.[17] V is the hybridization strength present in the SIM Hamiltonian.[16] Values for $CeMIn_5$ were obtained from inelastic neutron scattering [$M=$Co, $V\sim 0.5$ eV (Ref. 19)]. The parameter U is the on-site Coulomb repulsion between f electrons. Our best simulations yielded $U=1.5$ meV.

In the analysis of our data using the SIM, we have found that the simulations could not reproduce the peak at $\omega(T^*)$ for $CeCoIn_5$ for any realistic combination of g and r. The simulated curves always display a smooth softening on cooling below T^* illustrating the expected behavior within the Kondo single-impurity picture.

IV. CONCLUSION

We have presented Raman scattering spectra of the 1-1-5 heavy fermion family. Our results indicated that the characteristic Raman spectrum in the a,b plane consists of two modes at $\sim$38 and $\sim$165 cm^{-1} and a broad electronic background centered at low frequencies. We have analyzed in detail the T dependence of $CeCoIn_5$ and $LaCoIn_5$. The vibrational and electronic excitations in $CeCoIn_5$ present anomalies, and the changing behavior at T^* indicates a crossover in their electronic character, mainly due to hybridization effects. We showed that Nayak *et al.*'s model, which does not include the effects of magnetic correlations between the $4f$ electrons failed to reproduce the data, although it has successfully described the Raman data for magnetically ordered systems such as $CeAl_3$. This result may indicate a nontrivial renormalization of the electronic continuum below T^* where strong magnetic correlations between hybridized $4f$ electrons may play an important role. Interestingly, some features of our data seem to be qualitatively interpreted within the KG-KL scenario for $CeCoIn_5$. However, the lack of a microscopic theory describing the state of $CeCoIn_5$ below T^* does not enable us to reach any quantitative and/or definitive conclusions. The electronic continuum of $CeCoIn_5$ is hybridized to $4f$ electronic states and the strength of hybridization is temperature dependent. We found that the A_{1g} phonon with Fano line shape has special sensitivity to this hybridized state and it could be used to probe this state. Our results can be taken as a possible signature of the crossover among the two electronic regimes at T^* and bring a clear opportunity for modeling this behavior to gain additional insights into the T dependence of elementary excitations in the Kondo lattice. In particular, experiments involving the doping and pressure dependence of the Raman spectra of the 1-1-5 family could reveal more specific details about the microscopic nature of the correlated state below T^*.

ACKNOWLEDGMENTS

This work was supported by the Brazilian agencies FAPESP and CNPq and the U.S. DOE.

[1] Robert H. Heffner and Michael R. Norman, Comments Condens. Matter Phys. **17**, 361 (1996).
[2] P. W. Anderson, Phys. Rev. **124**, 41 (1961).
[3] B. Coqblin and J. R. Schrieffer, Phys. Rev. **185**, 847 (1969).
[4] V. T. Rajan, Phys. Rev. Lett. **51**, 308 (1983).
[5] See, for example, C. Rossel, K. N. Yang, M. B. Maple, Z. Fisk, E. Zirngiebl, and J. D. Thompson, Phys. Rev. B **35**, 1914 (1987).
[6] S. Nakatsuji, D. Pines, and Z. Fisk, Phys. Rev. Lett. **92**, 016401 (2004); S. Nakatsuji, S. Yeo, L. Balicas, Z. Fisk, P. Schlottmann, P. G. Pagliuso, N. O. Moreno, J. L. Sarrao, and J. D. Thompson, *ibid.* **89**, 106402 (2002).
[7] N. J. Curro, J. L. Sarrao, J. D. Thompson, P. G. Pagliuso, Š. Kos, At. Abanov, and D. Pines, Phys. Rev. Lett. **90**, 227202 (2003).
[8] C. Petrovic, R. Movshovich, M. Jaime, P. G. Pagliuso, M. F. Hundley, J. L. Sarrao, Z. Fisk, and J. D. Thompson, Europhys. Lett. **53**, 354 (2001); C. Petrovic, P. G. Pagliuso, M. F. Hundley, R. Movshovich, J. L. Sarrao, Z. Fisk, and J. D. Thompson, J. Phys.: Condens. Matter **13**, L337 (2001).
[9] V. A. Sidorov, M. Nicklas, P. G. Pagliuso, J. L. Sarrao, Y. Bang, A. V. Balatsky, and J. D. Thompson, Phys. Rev. Lett. **89**, 157004 (2002).
[10] A. Bianchi, R. Movshovich, I. Vekhter, P. G. Pagliuso, and J. L. Sarrao, Phys. Rev. Lett. **91**, 257001 (2003); A. Bianchi, R. Movshovich, C. Capan, P. G. Pagliuso, and J. L. Sarrao, *ibid.* **91**, 187004 (2003).
[11] E. J. Singley, D. N. Basov, E. D. Bauer, and M. B. Maple, Phys. Rev. B **65**, 161101 (2002).
[12] M. V. Klein, in *Light Scattering in Solids I*, edited by M. Cardona, Topics in Applied Physics, Vol. 8 (Springer-Verlag, Berlin, 1983), p. 147.

[13] A. Zawadowski and M. Cardona, Phys. Rev. B **42**, 10732 (1990).
[14] J. Menéndez and M. Cardona, Phys. Rev. B **29**, 2051 (1984).
[15] N. Harrison *et al.*, Phys. Rev. Lett. **93**, 186405 (2004).
[16] P. Nayak, B. Ojha, S. Mohanty, and S. N. Behera, Int. J. Mod. Phys. B **16**, 3595 (2002).
[17] D. Hall *et al.*, Phys. Rev. B **64**, 064506 (2001).
[18] H. Razafimandiby, P. Fulde, and J. Keller, Z. Phys. B: Condens. Matter **54**, 111 (1989).
[19] A. D. Christianson *et al.*, Phys. Rev. B **70**, 134505 (2004).